Optical-Model Analysis of Excitation Function Data and Theoretical Reaction Cross Sections for Alpha Particles

GEORGE IGO†
Los Alamos Scientific Laboratory, Los Alamos, New Mexico, Institute for Theoretical Physics, University of Heidelberg, and Max Planck Institute for Nuclear Physics, Heidelberg, Germany

(Received April 7, 1959)

The complex alpha particle-nuclear potential is determined with small uncertainty at the nuclear surface by experiments with alpha particles in the range of bombarding energies up to 50 Mev in conjunction with this optical-model analysis which assumes that the shape of the complex potential is exponential at the nuclear surface. The potential is given by the expression

$$V_\alpha+W_\alpha=\left\{-1100\exp\left[-\left(\frac{r-1.17A^{\frac{1}{3}}}{0.574}\right)\right]-45.7i\exp\left[-\left(\frac{r-1.40A^{\frac{1}{3}}}{0.578}\right)\right]\right\}\text{ Mev},$$

for values of r (in units of 10^{-13} cm) where the real part is $\gtrsim -10$ Mev. The elastic scattering data has been used to determine the potential. The calculated reaction cross sections are found to be in satisfactory agreement with excitation function data.

The total reaction cross section σ_R for alpha particles in the energy range 0–50 Mev on nuclei with charge $Z=10$, 20, 30, 50, 70, and 90 has been calculated using the potential $V_\alpha+iW_\alpha$ obtained from the analysis of elastic scattering data. The calculated values may be interpolated to obtain σ_R for other values of Z.

I. INTRODUCTION

ELASTIC scattering cross sections[1–10] and excitation functions[11–19] have been measured from many elements with alpha particles of bombarding energies ranging up to 50 Mev. The analyses[2,10,20–27] made so far have been only of the elastic scattering data. However, the optical-model calculations also predict the total reaction cross sections. These may be compared with the combined excitation functions for all possible reaction products as a further test on the optical-model potential obtained from elastic scattering data.

In practice, excitation functions are measured for only a few of the many possible reactions induced under alpha-particle bombardment. In many nuclei, however, these represent the bulk of the reaction cross section, and consequently the sum of the measured excitation functions can be compared with the reaction cross section calculations. A method[28] for measuring the *total* reaction cross section has been applied to proton-induced reactions.[28] No similar measurement for alpha particles has been reported so far. The results of this analysis suggest that excitation function data may also be valuable in optical-model analyses of reactions induced by protons, deuterons, etc.

II. ELASTIC SCATTERING

The elastic scattering of 18-Mev alpha particles from argon,[9] 40-Mev alpha particles from copper,[8] and 48-Mev alpha particles from lead[4] has been extensively analyzed in terms of the optical model.[26] In Figs. 1, 2, and 3, the experimental cross sections are plotted along with the best fits obtained from the optical-model analysis. The conclusion of this analysis was that the elastic scattering cross section is very sensitive to the surface of the real part of the nuclear potential. The results of earlier analyses are compatible with this statement. The real part V_α of the potential obtained

* Work performed under the auspices of the U. S. Atomic Energy Commission.

† Fulbright Fellow 1958–1959.

[1] G. W. Farwell and H. E. Wegner, Phys. Rev. **95**, 1212 (1954).
[2] Wall, Rees, and Ford, Phys. Rev. **97**, 726 (1955).
[3] Wegner, Eisberg, and Igo, Phys. Rev. **99**, 825 (1955).
[4] R. Ellis and L. Schecter, Phys. Rev. **101**, 636 (1956).
[5] H. E. Gove, Phys. Rev. **99**, 1353 (1955).
[6] Eisberg, Igo, and Wegner, Phys. Rev. **99**, 1606 (1955).
[7] E. Bleuler and D. J. Tendam, Phys. Rev. **99**, 1605 (1955).
[8] Igo, Wegner, and Eisberg, Phys. Rev. **101**, 1508 (1956).
[9] Seidlitz, Bleuler, and Tendam, Phys. Rev. **110**, 682 (1958).
[10] Kerlee, Blair, and Farwell, Phys. Rev. **107**, 1343 (1957).
[11] R. L. Walker, Phys. Rev. **76**, 244 (1949).
[12] I. Halpern, Phys. Rev. **76**, 248 (1949).
[13] S. N. Ghoshal, Phys. Rev. **80**, 939 (1950).
[14] K. G. Porges, Phys. Rev. **101**, 225 (1956).
[15] N. T. Porile, Bull. Am. Phys. Soc. Ser. II, **3**, 382 (1958).
[16] Bleuler, Stebbins, and Tendam, Phys. Rev. **90**, 460 (1953).
[17] E. Kelly and E. Segrè, Phys. Rev. **75**, 999 (1949).
[18] Vandenbosch, Thomas, Vandenbosch, Glass, and Seaborg, Phys. Rev. **111**, 1358 (1958).
[19] Glass, Carr, Cobble, and Seaborg, Phys. Rev. **104**, 434 (1956).
[20] J. S. Blair, Phys. Rev. **95**, 1218 (1954).
[21] N. Oda and K. Harada, Progr. Theoret. Phys. (Kyoto) **15**, 545 (1956).
[22] C. B. O. Mohr and B. A. Robson, Proc. Phys. Soc. (London) **A69**, 365 (1956).
[23] G. Igo and R. M. Thaler, Phys. Rev. **106**, 126 (1957).
[24] W. B. Cheston and A. E. Glassgold, Phys. Rev. **106**, 1215 (1957).
[25] J. S. Blair, Phys. Rev. **108**, 827 (1957).
[26] G. Igo, Phys. Rev. Letters **1**, 167 (1958).
[27] C. E. Porter, Phys. Rev. (to be published) and Phys. Rev. **99**, 1400 (1955).
[28] N. M. Hintz, *Proceedings of the University of Pittsburgh Conference on Nuclear Structure, 1957*, edited by S. Meshkov (University of Pittsburgh and Office of Ordnance Research, U. S. Army, 1957); R. M. Eisberg, *Proceedings of the International Conference on the Nuclear Model, 1959*, edited by A. E. S. Green, C. E. Porter, and D. S. Saxon (The Research Council, Florida State University).

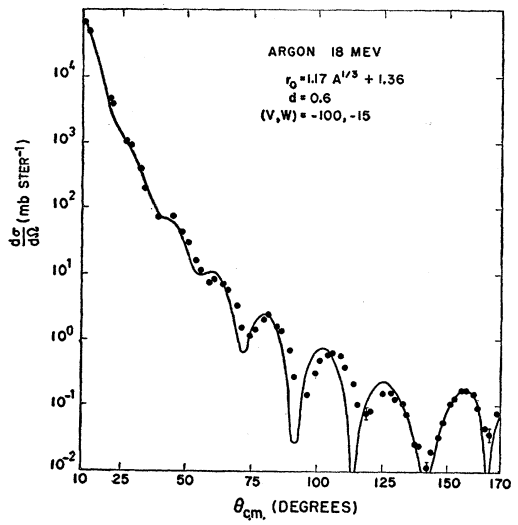

FIG. 1. Angular distribution of 18-Mev alpha particles elastically scattered from argon. The points are from the experiment of Seidlitz, Bleuler, and Tendam, multiplied by the factor 0.724. The solid curve is calculated using the parameters listed on the graph.

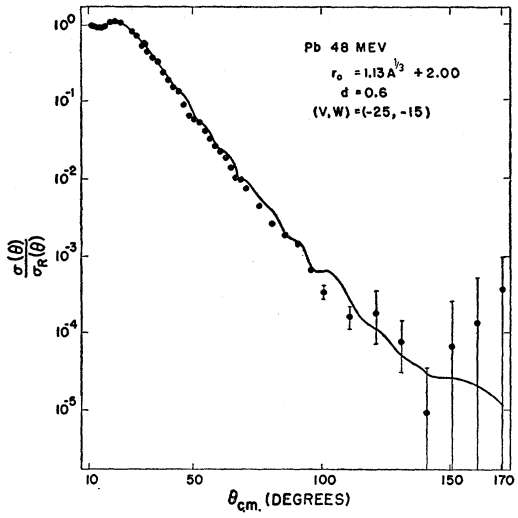

FIG. 3. Angular distribution of 48-Mev alpha particles elastically scattered from lead. The points are from the experiment of Schechter and Ellis. The solid curve is calculated using the parameters listed on the graph.

in this analysis could be represented as

$$-\{1100\exp[-(r-1.17A^{\frac{1}{3}})/0.574]\}\ \text{Mev}$$

for values $\gtrsim -10$ Mev with r in units of 10^{-13} cm.

In Figs. 4, 5, and 6, the real parts of the potential

$$(V+iW)/\{1+\exp[(r-r_0)/d]\},$$

obtained by varying the four parameters V, W, R_0, and d, are plotted for elastic scattering from argon at 18 Mev,[9] copper at 40 Mev,[8] and lead at 48 Mev,[4]

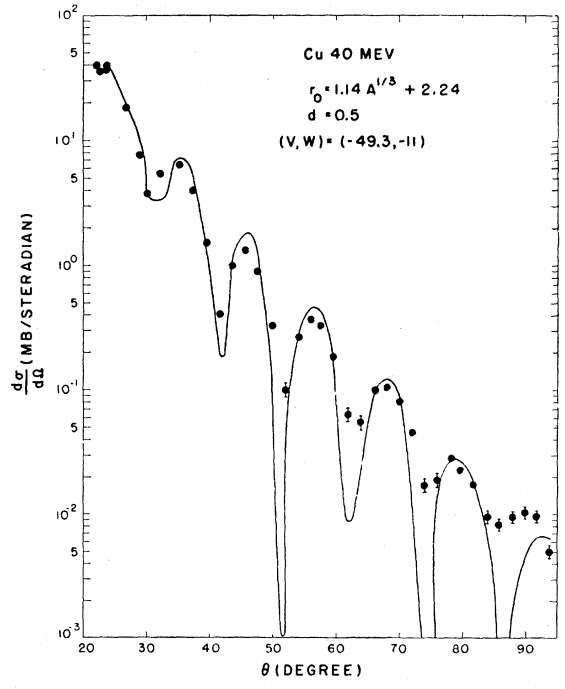

FIG. 2. Angular distribution of 40-Mev alpha particles elastically scattered from copper. The points are from the experiment of Igo, Wegner, and Eisberg. The solid curve is calculated using the parameters listed on the graph.

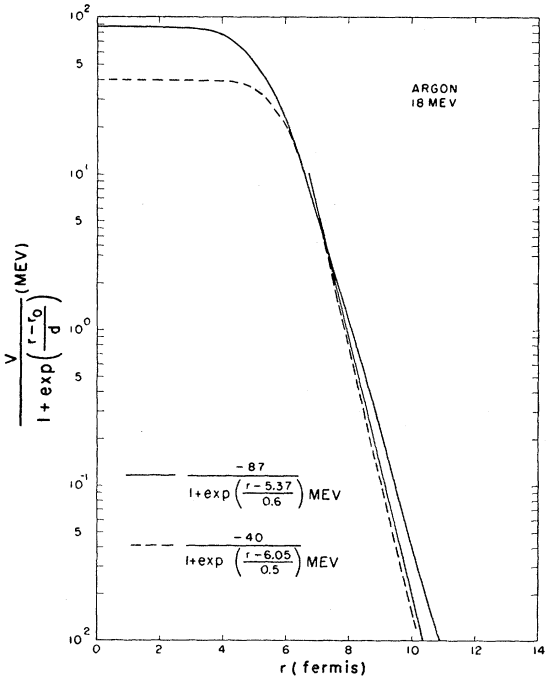

FIG. 4. The real part of the nuclear potential which best fits the elastic scattering data for 18-Mev alpha particles on argon plotted as a function of r in units of 10^{-13} cm. The potential $-1100\exp[-(r-1.17A^{\frac{1}{3}})/0.574]$ is also plotted.

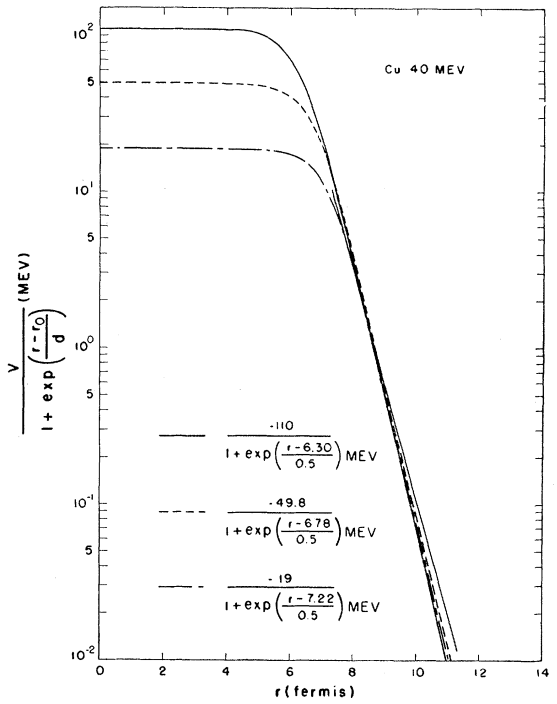

FIG. 5. The real part of the nuclear potential which best fits the elastic scattering data for 40-Mev alpha particles on copper plotted as a function of r in units of 10^{-13} cm. The potential $-1100\exp[-(r-1.17A^{\frac{1}{3}})/0.574]$ is also plotted.

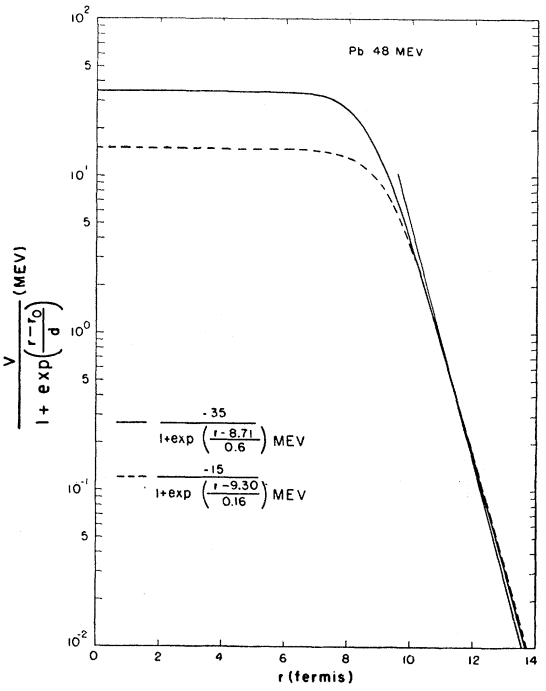

FIG. 6. The real part of the nuclear potential which best fits the elastic scattering data for 48-Mev alpha particles on lead plotted as a function of r in units of 10^{-13} cm. The potential $-1100\exp[-(r-1.17A^{\frac{1}{3}})/0.574]$ is also plotted.

respectively. Also plotted is V_α for argon, copper, and lead, respectively. Figures 7, 8, and 9 are real potentials at large values of r which yield relatively small residuals in the least squares analysis which is used as a criterion

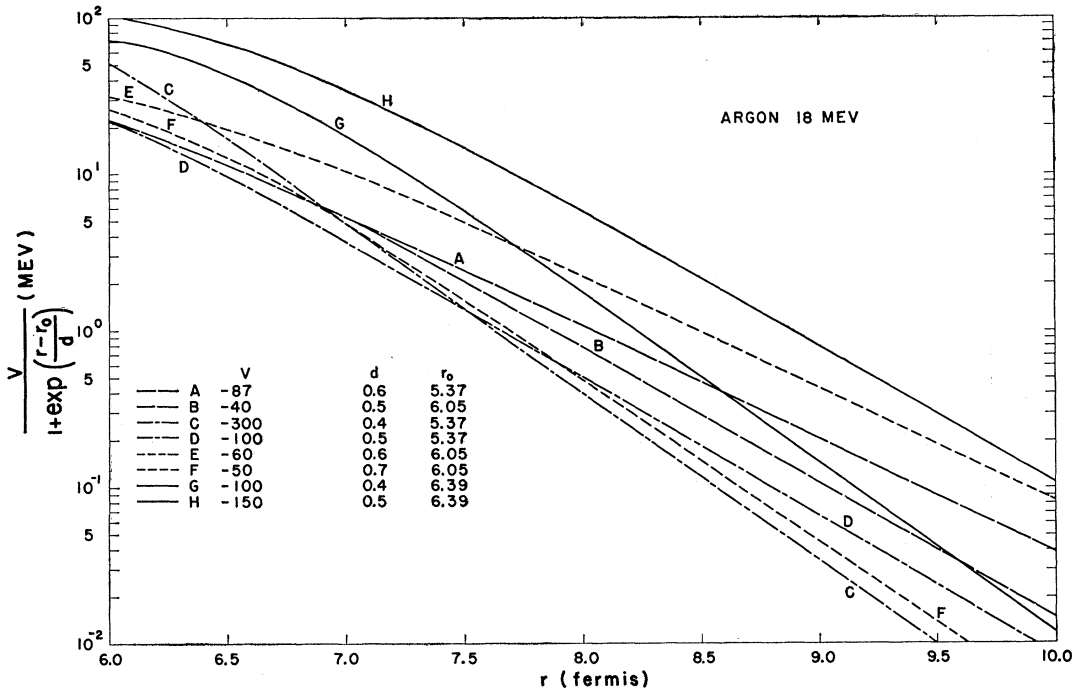

FIG. 7. Comparison of real potentials for the elastic scattering of 18-Mev alpha particles from argon. Curves A and B represent the best fits obtained (see Fig. 4). The remaining real potentials are lettered in order of increasing magnitude of the residuals obtained in the least-squares analysis used as a criterion for goodness of fit. The quantity V is in Mev; d and r_0, in 10^{-13} cm.

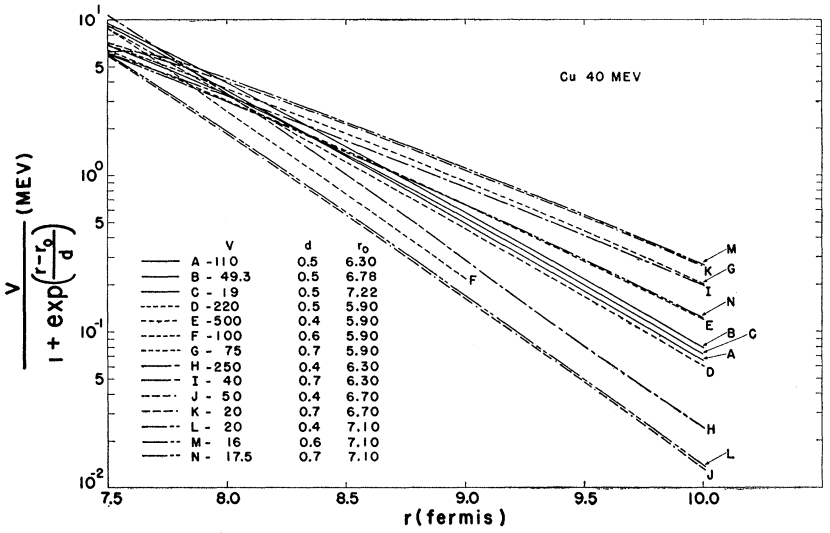

FIG. 8. Comparison of real potentials for the elastic scattering of 40-Mev alpha particles from copper. Curves *A*, *B*, and *C* represent the best fits obtained (see Fig. 5). The remaining real potentials are lettered in order of increasing magnitude of the residuals obtained in the least-squares analysis used as a criterion for goodness of fit. The quantity V is in Mev; d and r_0 in 10^{-13} cm.

for goodness of fit. The best fits (see Figs. 4, 5, and 6) lie close together. The remaining potentials deviate considerably from these best fits.

The imaginary part of the nuclear potential has also now been obtained and it may be expressed as

$$W_\alpha = -45.7 \exp[-(r-1.40A^{\frac{1}{3}})/0.578] \text{ Mev},$$

over the radial range where V_α is valid. In Figs. 10, 11, and 12, the best imaginary parts of the potential $(V+iW)/\{1+\exp[r-r_0)/d]\}$ are plotted for the three angular distributions. Also plotted is W_α for argon, copper, and lead, respectively. The imaginary parts of the potentials do not fall together as well at the surface of the potential as do the real parts. The potential

$$-(19+13i)/\{1+\exp[(r-7.22)/0.5]\} \text{ Mev}$$

(see Figs. 11 and 5) shows the largest deviation in the imaginary part (as well as in the real part). The angular distribution obtained from this potential does not fit the copper data as well as those obtained from the other potentials (the least-squares residual is five times as large as the best of the other two).

These results show that alpha-particle scattering defines the complex nuclear potential reasonably well at the surface, and are in accord with qualitative

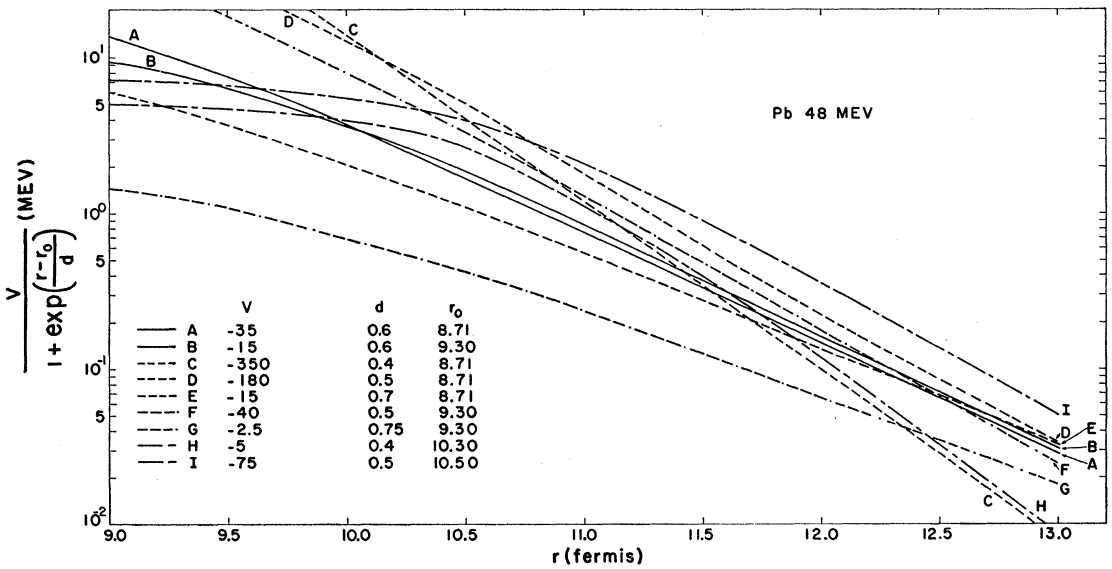

FIG. 9. Comparison of real potentials for the elastic scattering of 48-Mev alpha particles from lead. Curves *A* and *B* represent the best fits obtained (see Fig. 6). The remaining real potentials are lettered in order of increasing magnitude of the residuals obtained in the least-squares analysis used as a criterion for goodness of fit. The quantity V is in Mev; d and r_0, in 10^{-13} cm.

arguments made earlier by Ford and Wheeler.[29] These authors assumed that the mean free path of alpha particles in nuclear matter would be small. Consequently, the alpha particle would sample the potential at large values of r, where the Woods-Saxon potential[30] may be written approximately as

$$(V+iW)\exp[-(r-r_0)/d],$$

in agreement with the results of this analysis. Blair[25] has concluded, from an extensive analysis of alpha-particle data using the sharp-cutoff model,[20] that the scattering of alpha particles is primarily determined by the nuclear surface. Brussaard[31] has also concluded, from an application of the WKB method to the Schrödinger equation, that the scattering should be insensitive to the inner part of the potential.

III. EXCITATION FUNCTIONS

Total reaction cross sections have been calculated using the potential derived from the elastic scattering analysis,[32]

$$V_\alpha+W_\alpha=-1100\exp[(r-1.17A^{\frac{1}{3}})/0.574]$$
$$-47.5i\exp[-(r-1.40A^{\frac{1}{3}})/0.578].$$

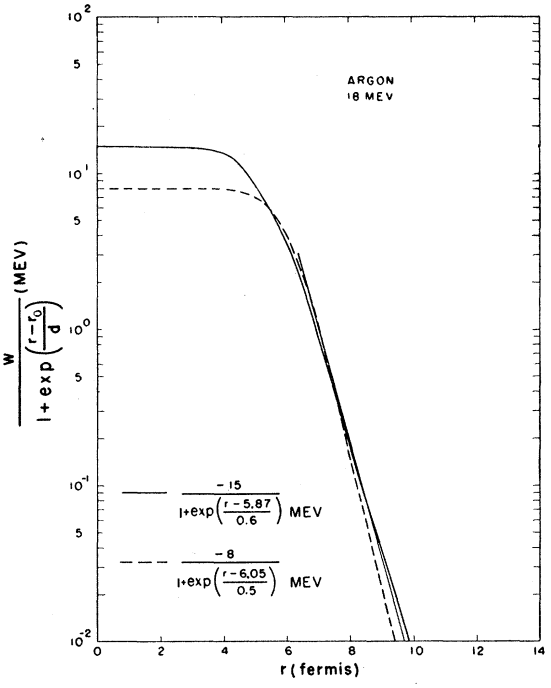

FIG. 10. The imaginary part of the nuclear potential which best fits the elastic scattering data for 18-Mev alpha particles on argon plotted as a function of r in units of 10^{-13} cm. The potential $-45.7\exp[-(r-1.40A^{\frac{1}{3}})/0.578]$ is also plotted.

[29] K. W. Ford and J. A. Wheeler (to be published).
[30] R. D. Woods and D. S. Saxon, Phys. Rev. **95**, 577 (1954).
[31] P. J. Brussaard, thesis, University of Leyden, 1958 (unpublished).
[32] See Part V for details on the calculation of total reaction cross sections.

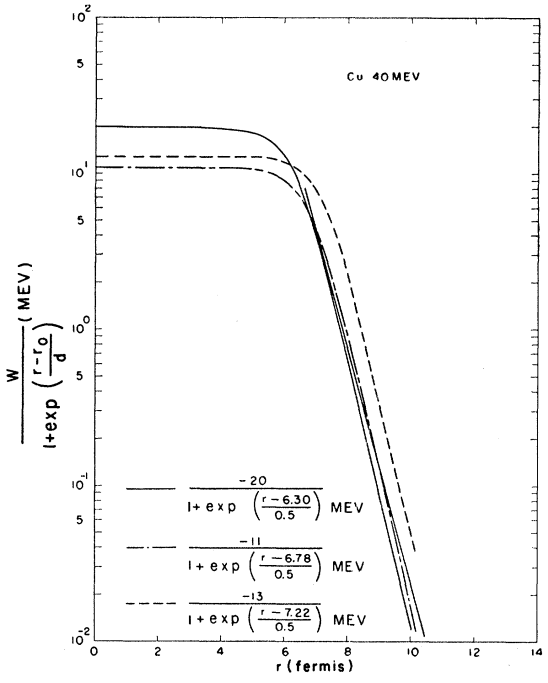

FIG. 11. The imaginary part of the nuclear potential which best fits the elastic scattering data for 40-Mev alpha particles on copper plotted as a function of r in units of 10^{-13} cm. The potential $-45.7\exp[-(r-1.40A^{\frac{1}{3}})/0.578]$ is also plotted.

Excitation function measurements where absolute cross sections exist have been made on isotopes of boron,[11]

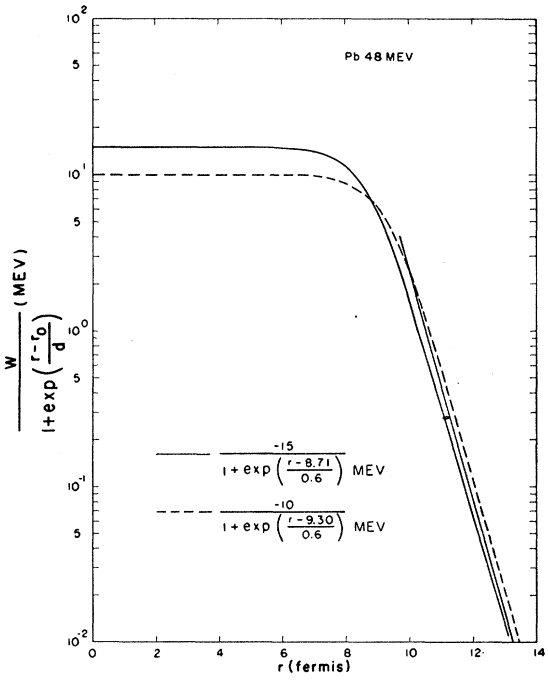

FIG. 12. The imaginary part of the nuclear potentials which best fits the elastic scattering data for 48-Mev alpha particles on lead plotted as a function of r in units of 10^{-13} cm. The potential $-45.7\exp[-(r-1.40A^{\frac{1}{3}})/0.578]$ is also plotted.

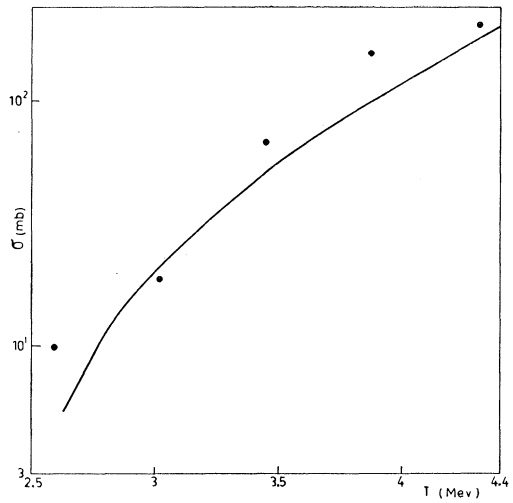

FIG. 13. The quantity σ_R calculated from the alpha-particle potential for magnesium. The points represent the trend of the (α,n) cross section on magnesium, multiplied by a factor to take into account the abundance of Mg^{25}.

beryllium,[12] magnesium,[12] aluminum,[12] nickel,[13] copper,[14] zinc,[15] silver,[14,16] bismuth,[17] uranium,[18] and plutonium.[19] The reaction cross sections can be compared with measurements of excitation functions for alpha-induced reactions if proper account can be taken of the contribution of reactions not measured in the experiments. For instance, the (α,p) reaction on aluminum is favored by a positive Q-value, whereas only the (α,n) excitation function[12] up to $T=4.5$ Mev has been measured. Consequently no quantitative comparison can be made. In the light elements ($A \lesssim 69$), the probability of proton emission F_p is reported large at $T \cong 20$ Mev.[33,34] Consequently, when excitation functions are missing for reactions where charged particles are emitted by light elements, it is impossible to make a quantitative comparison.[35] Some of these excitation functions are missing in the nickel[13] and copper[14] measurements. Here one can only note that the calculated cross sections are larger than the partial cross sections which are measured. Since it is very difficult to extrapolate the total reaction cross section σ_R to values of Z less than 10, no attempt was made to compare the calculations with the excitation functions of boron and beryllium.

In Fig. 13, σ_R for magnesium is compared with the excitation function measured by Halpern[12] for the (α,n) reaction on magnesium in the energy range $T=2.5$ to 4.4 Mev. In this experiment neutrons from the (α,n) reaction were measured to obtain an excitation function, and consequently the (α,n) reaction on all three isotopes of magnesium (78.47% Mg^{24}, 10.18% Mg^{25}, 77.47% Mg^{26}) could contribute to the measured neutron cross section. However the (α,p) reaction on Mg^{24} will account for most of the total reaction cross section in Mg^{24} in this energy range because of the large positive Q-values. The (α,n) and (α,p) reactions on Mg^{26} will be small because of the negative Q-values (-1.8 and -2.9 Mev, respectively) for this range of T. The (α,n) and (α,p) reactions on Mg^{25} have Q-values of 2.2 and -0.7 Mev, respectively. It is therefore apparent that the bulk of the observed neutrons are coming from the $Mg^{25}(\alpha,n)Si^{28}$ reaction. The experimental cross sections multiplied by a factor to take in account the relative abundance (10.18%) of Mg^{25} in natural magnesium are plotted also in Fig. 13. It should be noted that any contribution from the (α,n) reaction on Mg^{24} and Mg^{26} will decrease the values of the points plotted in Fig. 15, and bring them into better agreement with the calculation.

In Fig. 14, σ_R for zinc is plotted. The sum of the measurements of Porile[15] for the $(\alpha,\gamma)+(\alpha,2pn)+(\alpha,\alpha n)$

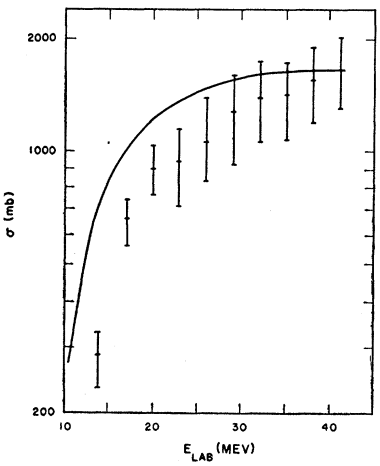

FIG. 14. The quantity σ_R calculated from the alpha-particle potential for zinc. The points are Porile's data on the total reaction cross section for alpha-induced reactions on Zn^{64}.

[33] B. L. Cohen and E. Newman, Phys. Rev. **99**, 718 (1955).
[34] Cohen, Newman, and Handley, Phys. Rev. **99**, 723 (1955).

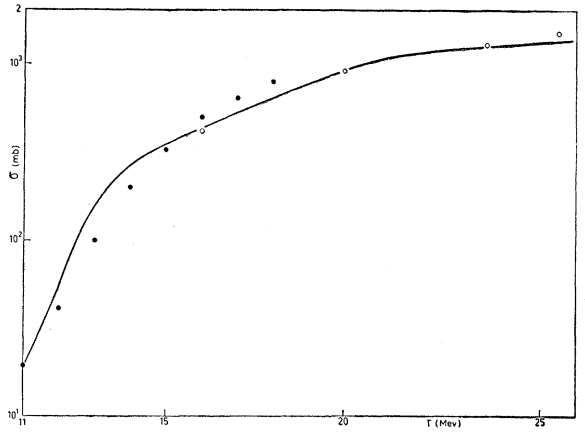

FIG. 15. The curve is σ_R calculated from the alpha-particle potential for silver. The solid circles, ●, are the sum of the (α,n) and $(\alpha,2n)$ cross sections. The open circles, ○, are the sum of (α,n), $(\alpha,2n)$, and (α,np) cross sections.

[35] See, for instance, J. M. Blatt and V. F. Weisskopf, *Theoretical Nuclear Physics* (John Wiley & Sons, Inc., New York, 1952), p. 365.

$+(\alpha,\alpha 2n)+(\alpha,\alpha pn)+\sum_{i=1}^{3}(\alpha,in)+\sum_{i=0}^{2}(\alpha,pin)$ excitation function on Zn^{64} plus the estimated contributions of the (α,γ) reaction for $T\gtrsim 18$ Mev and the $(\alpha,2p)$, $(\alpha,3p)$, $(\alpha,\alpha\gamma)$, $(\alpha,2\alpha)$, $(\alpha,\alpha p)$, $(\alpha,\alpha 2p)$ reactions is plotted. Porile[15] states that the errors indicated by the flags are mainly due to the uncertainty in estimating the magnitude of the latter contributions.

In Fig. 15, the experimental data of Bleuler *et al.*[16] on the $(\alpha,n)+(\alpha,2n)$ excitation function and of Porges[14] on the $(\alpha,n)+(\alpha,2n)+(\alpha,np)$ excitation function on Ag^{104} and σ_R for silver are plotted. The curve for σ_R is in satisfactory agreement with the experimental points.

In Fig. 16, the $(\alpha,2n)+(\alpha,3n)$ excitation function of Kelly and Segrè[17] and σ_R for bismuth are plotted in the energy range $T=24$ to 38 Mev. The discrepancy at 24 Mev is probably due to the absence of the (α,n) contribution to the total cross section.

In Fig. 17, the $(\alpha,f)+\sum_{i=1}^{5}(\alpha,in)+\sum_{i=0}^{3}(\alpha,pin)$, the $(\alpha,f)+\sum_{i=1}^{5}(\alpha,in)+(\alpha,p)+(\alpha,p2n)$, and the $(\alpha,f)+\sum_{i=1}^{3}(\alpha,pin)+(\alpha,\alpha n)$ excitation functions on U^{233}, U^{235}, and U^{238}, respectively, of Vandenbosch *et al.*[18] and σ_R for uranium in the energy range $T=18$ to 46 Mev are plotted. The quantity (α,f) is the fission reaction. The fit is considered satisfactory over the entire energy range.

In Fig. 18, the $(\alpha,f)+(\alpha,n)+(\alpha,2n)+(\alpha,4n)+(\alpha,pn)+(\alpha,p2n)$ and the $(\alpha,f)+\sum_{i=1}^{5}(\alpha,in)+(\alpha,pn)+(\alpha,p2n)+(\alpha,p3n)$ excitation functions Pu^{238} and Pu^{239} of Glass *et al.*[19] and σ_R for plutonium in the energy range $T=18$ to 48 Mev are plotted. The agreement between σ_R and the experimental points for Pu^{239} is satisfactory. Part of the difference between the total reaction cross section for Pu^{238} and Pu^{239} according to Glass *et al.*[19] is due to the missing (α,pn) reaction on Pu^{239}, which could not be measured.

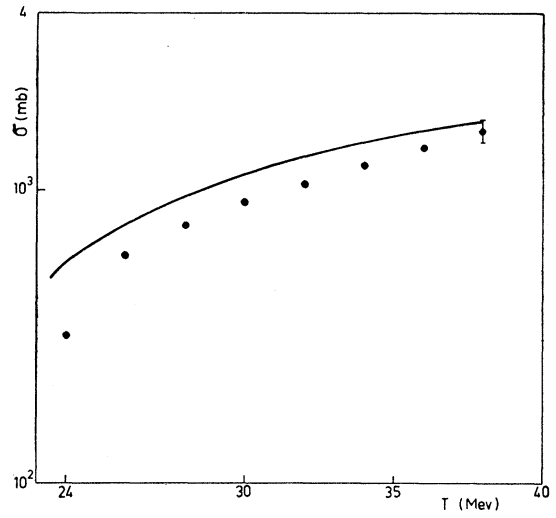

FIG. 16. The curve is σ_R calculated from the alpha-particle potential for bismuth. The points are the trend of the sum of the $(\alpha,2n)$ and $(\alpha,3n)$ cross sections on bismuth.

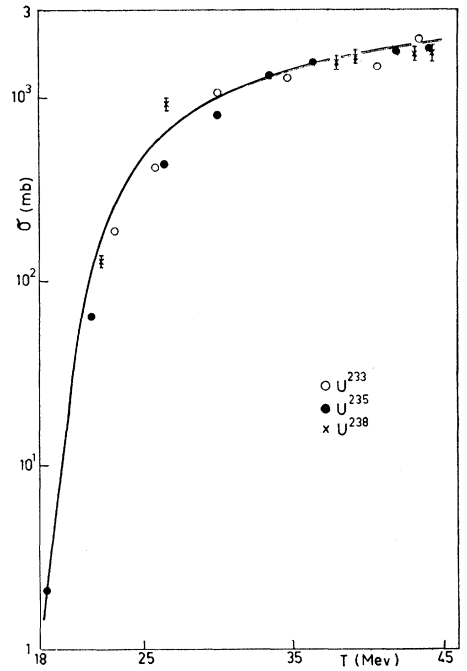

FIG. 17. The curve is σ_R calculated from the alpha-particle potential for uranium. The points are the sum of measured reaction cross sections for alpha-induced reactions on U^{233} (○), U^{235} (●), and U^{238} (×).

IV. REACTION CROSS SECTIONS FOR ENERGETIC ALPHA PARTICLES ON NUCLEI

Shapiro[36] and Feshbach and Weisskopf[37] have calculated the total reaction cross sections σ_R for protons,

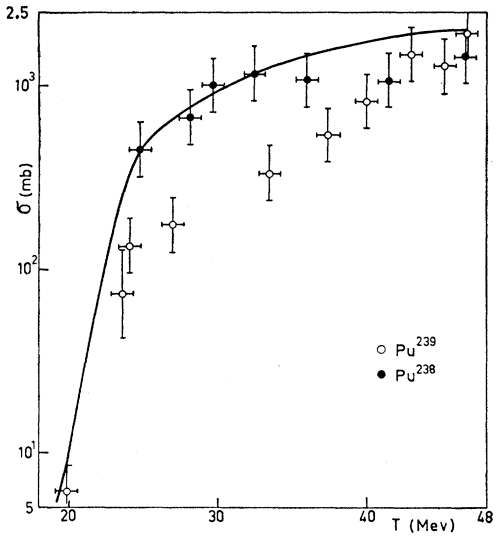

FIG. 18. The curve is σ_R calculated from the alpha particle potential for plutonium. The points are the sum of the measured reaction cross sections for alpha-induced reactions on Pu^{238} (●) and Pu^{239} (○).

[36] M. M. Shapiro, Phys. Rev. **90**, 171 (1953).
[37] J. M. Blatt and V. F. Weisskopf, *Theoretical Nuclear Physics* (John Wiley & Sons, Inc., New York, 1952), p. 352 and 491.

deuterons, and alpha particles using the schematic theory of nuclear reactions.[38] These authors have compared the shape of σ_R with excitation function measurements for alpha particles on Rh^{103},[39] Ag^{109},[39], aluminum,[12] magnesium,[12] and Bi^{209}.[17] They have found that the shape could be fit quite well with the radius parameter $1.3A^{\frac{1}{3}}\times10^{-13}$ cm, where A is the atomic number. Later measurements on other heavy nuclei where absolute reaction cross sections were measured disclosed that the radius parameter must be larger than $1.5A^{\frac{1}{3}}\times10^{-13}$ cm in order to fit the data.[16,14] Shapiro[40] and Blatt and Weisskopf[37] made calculations only for two values of the radial parameter, $1.5A^{\frac{1}{3}}\times10^{-13}$ cm and $1.3A^{\frac{1}{3}}\times10^{-13}$ cm (except for $Z<30$).[36] It has therefore been difficult to obtain quantitative fits to the excitation function data.

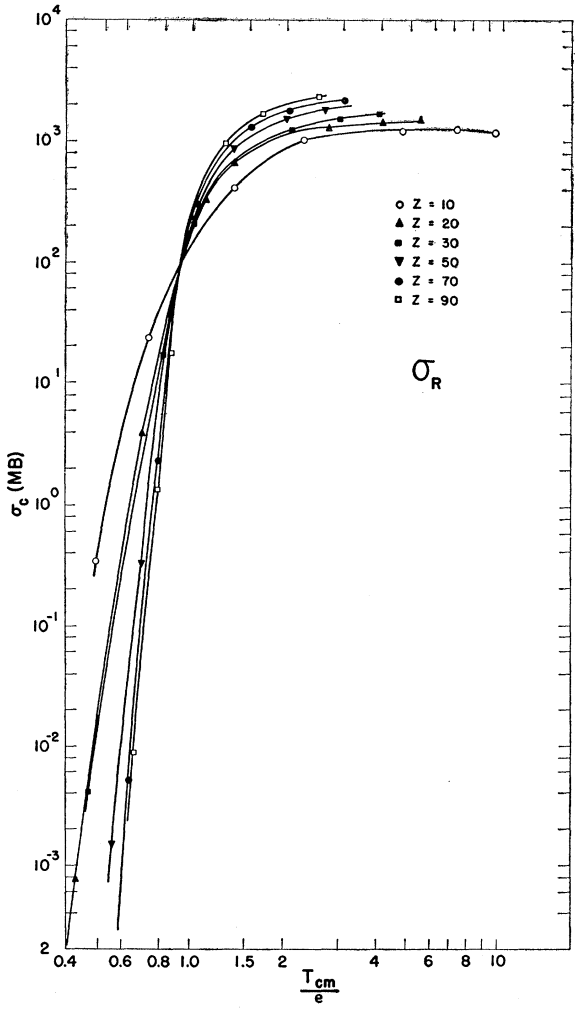

FIG. 19. The total reaction cross section *versus* T/e for $Z=10$, 20, 30, 50, 70, and 90.

[38] H. Feshbach and V. F. Weisskopf, Phys. Rev. **76**, 1550 (1949).
[39] D. J. Tendam and H. L. Bradt, Phys. Rev. **72**, 1118 (1947).

Another reason for interest in better values of σ_R is that σ_R enters into the calculation of energy level densities in the statistical theory of nuclear reactions.[40] According to the statistical theory, the energy level density $\rho(E_R)$ of the residual nucleus (after the emission of an alpha particle, for instance) at an excitation E_R is

$$\rho(E_R)dE_R=\text{const}\frac{N(E_0-E_R)dE_R}{(E_0-E_R)\sigma_c(E_0-E_R)},$$

where E_0 is the kinetic energy available to the alpha particle and residual nucleus in the center-of-mass system, when the residual nucleus is left in its ground state, and $N(E_0-E_R)d(E_0-E_R)=$number of nucleons emitted with energy between (E_0-E_R) and $(E_0-E_R)+d(E_0-E_R)$, where $T=E_0-E_R$ is the kinetic energy available in the center-of-mass system, and $(\sigma_cE_0-E_R)$ is the cross section for the formation of the compound nucleus for the inverse process. The interpretation of energy spectra of alpha particles emitted in (α,α'), (p,α), (d,α), etc. reactions is often made in terms of the statistical theory of nuclear reactions. To make a quantitative interpretation it is essential to have σ_R. The evidence presented in Part III shows that reliable values of σ_R can be obtained using the optical-model potential resulting from elastic scattering analysis.[26]

V. THE CALCULATION OF TOTAL REACTION CROSS SECTIONS

Total reaction cross sections have been calculated using the potential derived from the elastic scattering analysis,[26]

$$V_\alpha+iW_\alpha=-1100\exp\left[-\left(\frac{1-1.17A^{\frac{1}{3}}}{0.574}\right)\right]\text{Mev}$$
$$-45.7i\exp\left[-\left(\frac{r-1.40A^{\frac{1}{3}}}{0.578}\right)\right]\text{Mev},$$

for values of $V_\alpha\gtrsim-10$ Mev. The charge distribution determined by Ford and Hill[41] from the analysis of experiments[42] sensitive to the charge distribution parameters has been used. In the analysis of the data on elastic scattering of 40-Mev alpha particles, it was noted that the calculated cross section was not very sensitive to the shape of the charge distribution. The Coulomb potential due to the Hill-Ford charge distribution[30] is

$$\frac{Ze^2}{r_c}\left[\frac{1}{n^2}+\frac{1}{2}-\frac{x^2}{6}+\frac{e^{-n}}{n^2}\left(\frac{1-e^{nx}}{nx}+\frac{1}{2}e^{nx}\right)\right]\Big/$$
$$\left(\frac{1}{3}+\frac{2}{n^2}+\frac{e^{-n}}{n^3}\right),\quad x\leqslant1$$

[40] V. F. Weisskopf, Phys. Rev. **52**, 295 (1937).
[41] D. L. Hill and K. W. Ford, Phys. Rev. **94**, 1617 (1954).
[42] R. Hofstadter, *Annual Review of Nuclear Science* (Annual Reviews, Inc., Palo Alto, California, 1957), Vol. 7, p. 231.

TABLE I. Woods-Saxon potential parameters.

Z	A	V (Mev)	W (Mev)	r_0 (10^{-13} cm)	d (10^{-13} cm)	r_c (10^{-13} cm)	n
10	20	−50	− 6.27	$1.17A^{\frac{1}{3}}+1.77$	0.576	$1.17A^{\frac{1}{3}}$	4.4
20	40	−50	− 8.33	$1.17A^{\frac{1}{3}}+1.77$	0.576	$1.17A^{\frac{1}{3}}$	5.5
30	65	−50	−10.5	$1.17A^{\frac{1}{3}}+1.77$	0.576	$1.17A^{\frac{1}{3}}$	6.5
50	119	−50	−15.1	$1.17A^{\frac{1}{3}}+1.77$	0.576	$1.17A^{\frac{1}{3}}$	8.0
70	173	−25	− 9.57	$1.17A^{\frac{1}{3}}+2.17$	0.576	$1.17A^{\frac{1}{3}}$	9.0
90	232	−25	−12.2	$1.17A^{\frac{1}{3}}+2.17$	0.576	$1.17A^{\frac{1}{3}}$	10.0

and

$$\frac{Ze^2}{r_c}\left[\frac{1}{x}-e^{n-nx}\left(\frac{1}{x}+\frac{n}{2}\right)\right]\Big/\left(e^{-n}+2n+\frac{n^3}{3}\right), \quad x\geqslant 1$$

where

$$x=r/r_c,$$

and where n is 10 for heavy elements and is proportional to $A^{\frac{1}{3}}$. Large values of n (10) give charge distributions approximately constant for small values of r; small values, exponential charge distributions. The quantity r_c is the distance out to the half-value point of the charge distribution. The value $1.17A^{\frac{1}{3}}\times 10^{-13}$ cm was chosen larger than the value obtained from the electron scattering experiments[42] to take roughly into account the effect of the finite size of the alpha-particle charge distribution.

The parameters V, W, r_0, and d listed in Table I for the Woods-Saxon[30] potential

$$(V+iW)\Big/\left[1+\exp\left(\frac{r-r_0}{d}\right)\right]$$

have been chosen to reproduce $V_\alpha+iW_\alpha$ for values of r where the real part of the potential $\gtrsim -10$ Mev. The depth of the potential for small values of r is also fixed when the parameters in Table I are used although it has been shown[26] that alpha-particle scattering is not sensitive to the depth. This procedure was necessary in order to use the existing calculational program.

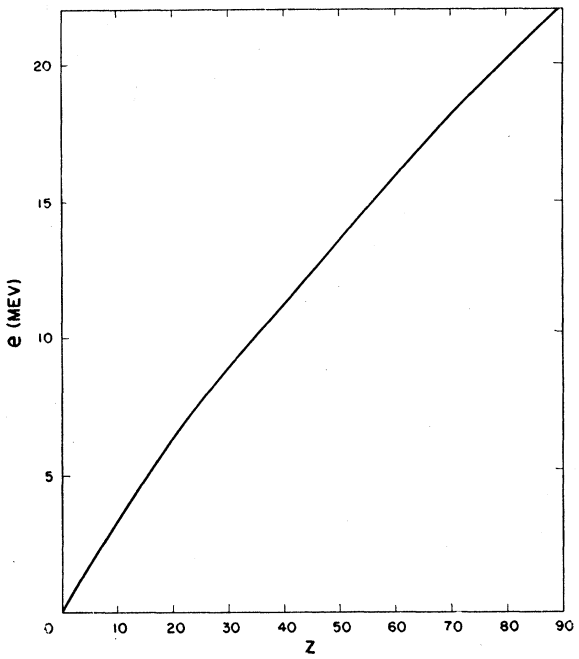

FIG. 20. The quantity e *versus* Z; e has been calculated using the parameters listed in Table II.

Table II lists the calculated values of the total reaction cross sections using the parameters listed in Table I. The quantity T is the kinetic energy in the center-of-mass system, and e is the maximum height of the potential barrier for $l=0$ alpha particles. Figure 19 is a plot of σ_R *versus* T/e. It is relatively easy to interpolate between the calculated cross sections for intermediate values of Z using Fig. 19. The quantity e is plotted *versus* Z in Fig. 20 where e has been calculated using the parameters listed in Table II.

TABLE II. Total reaction cross sections, σ_R.

Z	10			20			30		
e(Mev)	3.33			6.34			8.97		
	T (Mev)	σ_R (millibarns)	T/e	T (Mev)	σ_R (millibarns)	T/e	T (Mev)	σ_R (millibarns)	T/e
	33.3	1176.9	10.0	36.4	1465.4	5.73	37.7	1655.0	4.20
	25.0	1231.2	7.50	27.3	1426.0	4.30	28.2	1528.8	3.14
	16.7	1219.6	5.01	18.2	1286.5	2.86	18.8	1230.8	2.095
	8.33	1038.0	2.50	9.09	659.3	1.43	9.42	200.14	1.05
	4.77	419.42	1.43	7.28	322.6	1.147	7.52	16.56	0.838
	2.50	23.74	0.750	4.54	3.852	0.715	4.71	0.00419	0.523
	1.67	0.3461	0.502	2.73	0.000762	0.430			
Z	50			70			90		
e(Mev)	13.76			18.15			22.06		
	T (Mev)	σ_R (millibarns)	T/e	T (Mev)	σ_R (millibarns)	T/e	T (Mev)	σ_R (millibarns)	T/e
	38.7	1809.7	2.81	58.7	2184.0	3.23	59.0	2316.6	2.67
	29.0	1521.9	2.11	39.1	1783.1	2.15	39.3	1692.8	1.78
	19.35	871.5	1.408	29.3	1309.4	1.61	29.5	920.4	1.335
	14.50	230.9	1.053	19.55	307.64	1.075	19.7	17.14	0.891
	9.68	0.327	0.704	14.68	2.333	0.807	17.7	1.3055	0.804
	7.73	0.001542	0.562	11.70	0.00526	0.643	14.75	0.00893	0.667
	4.84	0	0.352						

VI. SUMMARY

The conclusion reached earlier[26] and discussed in detail in this paper, that alpha-particle elastic scattering is sensitive to the potential surface, is strengthened by this analysis of excitation function data. The reaction cross sections *versus* bombarding energy obtained from $V_\alpha+iW_\alpha$ have been compared with alpha-induced excitation functions.[12,14–18] When proper account is taken of missing reactions, i.e., alpha-induced reactions on a particular nuclide which have not been measured, the excitation functions measure the total reaction cross section as a function of bombardment energy. The agreement with the excitation function data strengthens the conclusion reached from the elastic-scattering analysis.

Qualitative arguments can be made to account for the conclusion stated above. Ford and Porter[27] make a "brick wall" argument to suggest a short mean free path for complex nuclear structures such as the alpha particle in nuclear material. Rasmussen[43] has emphasized the importance of the exclusion principle in alpha-particle interactions, namely that at these bombarding energies the alpha particle as an entity is probably excluded from the center of the nucleus. A possible way to treat the optical model taking into account the exclusion principle has been suggested recently by Frantz *et al.*[44]

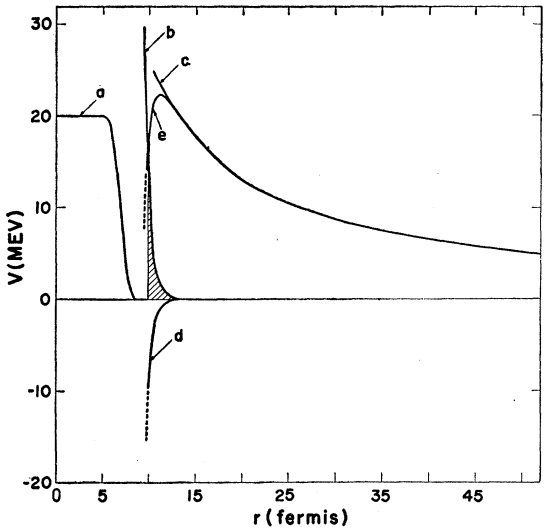

FIG. 21. Curves *a* and *b* are the form factor for the charge distribution of uranium (curve *b* is a scaled-up section of curve *a*). Curves *c* and *d* are the Coulomb potential for $Z=92$ and the real part of the alpha particle-nuclear potential, respectively. Curve *e* is the real part of the potential for an $l=0$ alpha particle. The shaded area is discussed in the text.

[43] J. O. Rasmussen, Revs. Modern Phys. **30**, 424 (1958).
[44] Frantz, Mills, Newton, and Sessler, Phys. Rev. Letters **1**, 340 (1958).

Some rough conclusions can be drawn concerning the alpha decay of heavy nuclei. In Fig. 21 the real part of the total potential obtained from this analysis (curve *e*) is compared with the charge distribution[45] (curves *a* and *b*) for uranium (curve *b* is a scaled-up section of curve *a*). The neutron distribution is assumed to be equal to the charge distribution. The present analysis indicates that the elastically scattered alpha particles do not penetrate to depths appreciably greater[46] than $r=9.9$ fermis in the uranium nucleus, since the scattering is not sensitive to the real part of the potential at smaller values of r. In alpha decay, alpha-particle clusters formed at smaller values of r would dissolve before they could penetrate the Coulomb barrier. The probability of finding two neutrons and two protons beyond $r=9.9$ fermis (the hatched area in Fig. 21) is of the order of 0.02%. This must be considered a qualitative result for several reasons. First, no account has been taken of the effect of surface deformations. Rasmussen and Segall[47] point out that the alpha-particle wave functions must be nonuniform on the surface of a spheroidally deformed nucleus in order to account for measured alpha-particle decay intensities. In addition it should be noted that the electron scattering results are not very sensitive to the exact shape of the tail of the charge distribution.[45]

ACKNOWLEDGMENTS

It is a pleasure to acknowledge discussions concerning alpha-particle reactions with Professor K. W. Ford, Dr. D. L. Hill, Professor J. H. D. Jensen, Dr. C. Porter, Professor J. O. Rasmussen, Dr. R. M. Thaler, and with the participants of a conference on the optical model which was held at Los Alamos last year. Thanks are particularly due Dr. D. L. Hill for a great deal of encouragement and for making arrangements for using the facilities at the Los Alamos Scientific Laboratory. In this connection thanks are also due Professor A. E. S. Green. Thanks are due Professor R. Sherr and Professor E. M. Henley for critical comments concerning the manuscript.

[45] Hahn, Ravenhall, and Hofstadter, Phys. Rev. **101**, 1131 (1956).
[46] Dr. I. E. McCarthy has kindly informed me in advance of publication of his calculations using the optical-model potentials discussed in this paper for the elastic scattering of 18-Mev alpha particles from argon. He finds that the alpha-particle flux decreases rapidly towards the center of the nucleus, but remains finite at the center. The present analysis and the experimental data evidently are not sufficiently precise to reflect the "sampling" of the nuclear interior by the alpha particle.
[47] J. O. Rasmussen and B. Segall, Phys. Rev. **103**, 1298 (1956).